Determination of Picogram Quantities of Rare-Earth Elements in Meteoritic Materials by Direct-Loading Thermal Ionization Mass Spectrometry

N. Nakamura,*[1] K. Yamamoto, S. Noda, Y. Nishikawa, H. Komi, H. Nagamoto, and T. Nakayama

Department of Earth Sciences, Faculty of Science, Kobe University, Nada, Kobe 657, Japan

K. Misawa[2]

Department of Science of Material Differentiation, Graduate School of Science and Technology, Kobe University, Nada, Kobe 657, Japan

A procedure for direct-loading isotope dilution mass spectrometry (DL-IDMS) of rare-earth elements (REE), alkaline-earth metals (Mg, Ca, Sr, and Ba), alkali metals (K and Rb), and iron in microcomponents of meteorites is described. Without chemical separation the acid-decomposed sample was directly loaded onto a mass spectrometer filament and subjected to thermal ionization mass spectrometry with careful control of the filament current and the oxygen partial pressure. This technique permits, on a routine basis, precise concentration determinations of individual REE at the levels of $>10^{-13}$ g (or $>10^{-15}$ mol) in meteoritic and terrestrial materials such as chondrules, mineral fragments, and basaltic samples. The results demonstrate the presence of highly fractionated REE in microcomponents of meteorites, which indicates a new chemical aspect of REE in the early planetary materials. The DL-IDMS technique can thus be used as the only means of high-precision analyses of small planetary materials with low REE contents.

The thermal ionization isotope dilution mass spectrometry (IDMS) has been in current use for precise determination of rare-earth element (REE) concentrations in terrestrial, lunar, and meteoritic materials (*1–4*). The application of this technique, however, is normally limited to milligram or larger sizes of silicate samples. There exist two main problems for the application. First, interferences of major elements to the stability and efficiency of ionization of REE occur during the thermal ionization mass spectrometry if a clean chemical separation of REE from major elements is not performed (hereafter called the "matrix problem"). Second, there is the long-recognized problem of multiple isobaric interferences among REEs. Hence, to eliminate the interferences, acid decomposition of samples and chemical separations of REE from major elements and of light from heavy REE are common practice in using the IDMS technique. Then the processes result in contributions of sometimes considerable amounts of procedural blanks to the samples, which may lead to unrealistic data, particularly in the case of small samples with low REE levels. Hence, the technique has rarely been applied to analyses of REE in submilligram size samples.

The detailed REE abundance features of fine planetary materials, typically chondrules and inclusions in chondrites, have increasingly caught the attention of cosmochemists. The neutron activation analysis (NAA) techniques (e.g. ref 5–7) and more recently the ion-probe technique (*8*, *9*) have been successfully applied to obtain REE characteristics of small planetary materials. However, the NAA data do not necessarily give us detailed information on REE fractionations for the materials with low REE contents, and the ion probe technique is still of limited use.

It was demonstrated that direct-loading thermal ionization mass spectrometry allowed the precise isotopic measurement of Ca and Mg in a reduced amount of material (*10*). In this work, we have initiated application of this technique to isotope dilution analyses of refractory trace elements REE in meteoritic and terrestrial materials and established the method that permits, on a routine basis, precise analyses of individual REE at the levels of $>10^{-13}$ g ($>10^{-15}$ mol). The purposes of this report are to describe the newly developed direct-loading isotope dilution mass spectrometry (DL-IDMS) technique of determining REE and other elements and to demonstrate precise analyses of chondrules and mineral fragments from meteorites by using this technique.

EXPERIMENTAL SECTION

The general analytical scheme for meteorite samples is shown in Figure 1. Chondrules or mineral fragments were broken roughly into two parts within a clean agate mortar. One fragment was used for the thin section preparation, petrographic examinations, and major element analyses by an electron probe microanalyzer (EPMA). The other half (normally 10–500 μg) was subjected to IDMS analyses. The U.S. Geological Survey standard rock BCR-1 was also analyzed by the same IDMS techniques.

(1) Spikes. At the early stage of this work, we had only one composite REE spike solution but later two more spike solutions (Ba–Sr–Rb–K and Ca–Mg–Fe composite solutions) were prepared. Spike isotopes used are shown in Table II. (All the enriched isotopes were obtained from Oak Ridge National Laboratory.) During the course of this work we have examined isotopic compositions of Rb, Sr, Sm, Nd, and Yb spikes. The isotopic abundances of spike isotopes observed by us were in agreement within 0.1% with those given by Oak Ridge National Laboratory. All analyses for meteorite samples were carried out by using the same REE composite spike solution as used in our previous works (*11–14*) and thus there should be no systematic biases between this work and our previous works due to spike calibration. A new REE composite spike solution was prepared in this work and was used for analyses of BCR-1 standard to test the consistency of the isotope dilution analyses with and without chemical separation and to compare them with REE data from other institutions.

(2) Blanks. All reagents used were purified carefully (see footnotes of Table I). The impurities of REE and other trace elements in reagents and procedural blanks have been repeatedly checked during the course of this work. It is pointed out that the total processing blanks of DL-IDMS are much higher than the sum of the amounts of impurities in reagents used (2–5 μL of $HClO_4$, HF, and HNO_3 for submilligram samples). It turned out that the major source of blanks (in DL-IDMS) was the Teflon bomb used for sample decomposition. Hence, the cleaning procedures for bombs are quite important to lower blank levels. For cleaning, decomposition bombs were cooked with a hot HF–HNO_3

[1] Also affiliated with Department of Science of Material Differentiation, Graduate School of Science and Technology, Kobe University.

[2] Present address: Institute for Cosmic Ray Research, University of Tokyo, Tanashi, Tokyo 188, Japan.

0003-2700/89/0361-0755$01.50/0

Table I. Impurities in Reagents[a] and Blanks during Chemical Processes

	reagent impurities, 10^{-12} g/g						procedural blanks, 10^{-12} g	
	H_2O	HCl	HNO_3	$HClO_4$	HF	Ca–Mg[b]	DL-IDMS	normal IDMS[c]
La	0.4	2	0.68	4	3.6	4.5	1–3	3.3
Ce	0.66	4	0.86	6.2	2.2	7.9	0.7–2.5	–
Nd	0.29	0.6	0.38	1.9	0.12	3.0	0.2–1.5	2.0
Sm	0.033	0.15	0.04	0.36	0.64	–	0.05–0.35	0.36
Eu	0.006	0.03	0.05	0.10	1.2	0.3	0.02–0.13	0.13
Gd	–	0.12	0.07	0.40	0.22	0.8	0.08–0.1	–
Dy	–	0.11	0.19	0.38	0.29	–	0.10	0.51
Ru	–	–	–	–	–	–	–	0.39
Yb	–	–	–	–	–	–	0.39	–
Lu	0.003	0.03	–	–	–	0.4	0.02–0.09	0.093
Ba	4.7	14	17	38	16	900	23–140	
Sr	1.4	7	7.6	18	21	83	0.7–8	
Rb	0.24	0.8	0.67	3.1	5.5	5.4	0.1–0.3	
K	140	220	390	980	1900	4500	90–260	

[a] Reagents used were purified by the following methods: H_2O, water deionized with cation exchange resin was distilled with a Pyrex apparatus and then sub-boiled by using a quartz apparatus; HCl (6 M), pure HCl gas was bubbled into water; HNO_3 (15 M), distilled with a Pyrex apparatus and then sub-boiled twice with a quartz apparatus; HF (24 M), bottle to bottle sub-boiled 4 times; $HClO_4$ (14 M), sub-boiled 4 times with a quartz apparatus. [b] The Ca–Mg–Fe composite spike solution. [c] Total procedural blanks for a few milligram size samples (*13*) which include blanks for chemical separation of REE using cation exchange resin columns. Blanks for samples with larger sizes are similar or better than those given in ref 23.

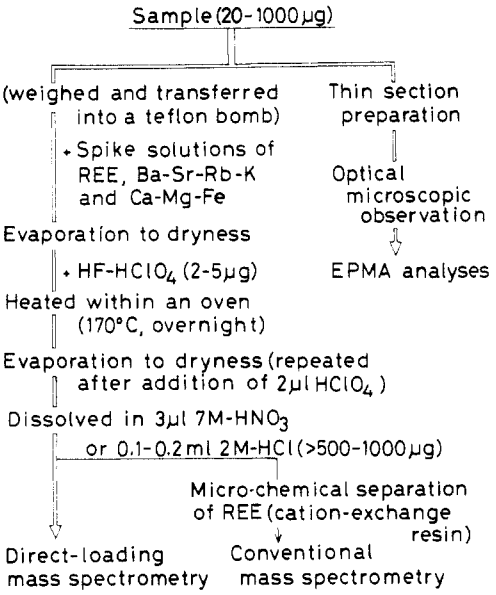

Figure 1. Schematic illustration of analytical procedures.

mixture solution for a few days and with hot HCl for a few hours and then were washed with water. The bombs were further cleaned with an HF–$HClO_4$ mixed solution at 170 °C in an oven (overnight) before using.

Caution was also taken against cross-contamination (specifically of Ba and K) from Ca–Mg–Fe spike solution to other spike solutions or samples. In Table I, the procedural blanks do not include blanks from spike solutions. In view of significantly high impurities, only the minimum quantity of Ca–Mg–Fe spike solution (1–2 drops ≤30 mg) was used for samples smaller than 50 μg. Blanks from other spike solutions were negligibly small. Total contributions of REE blanks including spike solutions to sample were less than several percent for ≥20 μg size samples but significantly large for smaller samples.

(3) Decomposition Procedures. Samples less than a few milligrams were weighed with a microbalance (precision = ±1 μg) using an aluminum foil vessel and transferred into a small (1.5 mL) homemade Teflon bomb. Spike solutions were added one by one to the sample. After evaporation of spike solutions to dryness, 2–5-μL quantities of 24 M HF and 14 M $HClO_4$ (or 15 M HNO_3) were added to it. The Teflon bomb (with a snap-on cover) containing the sample was sealed in a stainless steel container at 170 °C within an oven overnight. After heating, the sample solution was evaporated to dryness. The complete decomposition of the sample was confirmed with a binocular microscope. Chondrules, matrix, and mineral fragments were easily decomposed by this method. In a few cases beside this work, however, undecomposed ingredients were noted in samples after the above treatment. In such cases, the decomposition procedures must be repeated. Every step of the above procedures was cautiously executed to ensure the equilibration of isotope tracers with samples.

Depending on sample sizes and the REE concentration levels expected from petrographical examinations (and EPMA analyses when available), the acid-decomposed sample was subjected to DL-IDMS or normal IDMS procedures. Normally, samples smaller than 1 mg were loaded in HNO_3 directly on a Ta side filament for a double-filament or a Re filament for single-filament arrangement, evaporated at <1 A in air, and then measured by DL-IDMS. On the other hand, if samples were larger than 1 mg (or 0.5 mg in the case of sample with much higher REE contents than chondritic levels), the samples were subjected to dissolution in 0.1–0.2 mL 2 M HCl solution, chemical separation of REE using a cation exchange resin column and normal IDMS basically similar to those of Nakamura (*15*, *16*).

In this work, the alkali and alkaline-earth metals were analyzed by DL-IDMS in spite of the sample size. We did not have too much difficulty in using DL-IDMS for these elements.

(4) Mass Spectrometry. We used a JMS-05RB solid source mass spectrometer (Japan Electron Optics Laboratory) equipped with a 30 cm radius analyzer, a collector system (multiplier and Faraday cup) (*17*), and an on-line personal computer. The isotopic measurements in this work were carried out by a peak-scanning method using the collector system consisting of a 14-stage electron multiplier (gain = 1×10^4 at 2 kV) and a vibrating reed electrometer (ADVANTEST TR8401). An oxygen (or air) pressure regulator is attached to the source chamber in order to control the oxygen partial pressure and facilitate the analyses of LaO^+, GdO^+, and other oxides. The advantages of this system have been discussed by Schumann et al. (*18*).

(a) Filament and Ion Source. Marz grade Re (purity 99.996%) and VP grade Ta filaments (both filaments 0.0008 in. thick and 0.03 in. wide) (Material Research Corp.) were used in this work. Filaments were outgassed at 4.2 Å for Re and 3.5–3.8 Å for Ta for 30–60 min. Impurities of REE and other elements in outgassed filaments of our interest were found to be below the detection limits under run conditions. However, when a VP grade Re filament was used for small samples, clearly misleading results were obtained for Ba and Ce (and possibly La) concentrations due to filament impurity. Hence, we have not used this type of filament in DL-IDMS for meteorite analyses.

The thermal ionization was carried out by use of double- and single-filament ion sources (double filament, (side) Ta, (center) Re; single filament, Re). In a few cases of DL-IDMS (such as with

an extremely small sample like Khohar matrix [Table IV]), samples were loaded on both center and side filaments and subjected to a combined single–double filament mass spectrometry.

(b) Isotopic Measurement and Precision. The isotopic ratios were measured by scanning the mass range of two to four isotopes including spike and monitor isotopes. The scanning sequences were cycled normally 3–5 times and data were taken in sets of five to nine ratios (one cycle scanning of two REE isotopes needs 1 min). In general, this data acquisition process was repeated after raising the filament current several times for every element. The mean isotopic ratios were calculated for several blocks (30–100 ratios). For normal mass spectrometry, 2 times the standard deviation of the mean was 0.1% or smaller at the intensity of 10^{-8} A (at the vibrating reed electrometer current). For analyses of 20–50 μg size meteorite samples by DL-IDMS, the intensities at the detector range from 10^{-8} A for K to 10^{-11} A for Yb (see Table II). The precisions of isotopic analyses on these samples were 0.1–0.5% for most elements but 0.2–1% (up to 2%) for heavy REE.

Small instrumental mass fractionations can occur during isotopic measurements. But isotopic shift due to mass fractionation was normally too small to detect clearly but was recognized after significant vaporization of elements. Isotopic data with large mass fractionations were discarded and only isotopic data with no or small (<0.3%) fractionations were employed for concentration calculations without mass fractionation corrections. It seems that compared with conventional mass spectrometry, direct-loading run does not yield larger mass fractionations.

RESULTS AND DISCUSSION

As mentioned later, DL-IDMS analysis of REE in meteoritic materials was initiated in order to detect any specific component with Ce enrichment in the Khohar meteorite. After tough struggles to many problems specific to "direct-loading" mass spectrometry, the technique was established and has been used routinely to analyze REE in microcomponents of meteorites in this laboratory (*11–13*). The following are discussions on major problems of the DL-IDMS technique, analytical precisions, and results on the terrestrial basalt standard BCR-1 and meteoritic materials.

(1) Matrix Problem in DL-IDMS. At the early stage of DL-IDMS work, we met with difficulties in obtaining sufficient ionization efficiency of REE. We recognized that the ionization efficiency of REE is much lower than expected from normal mass spectrometry for all temperature ranges and then found that if the intensity ratios of major element ions (e.g. Na^+ and Ca^+) to REE ions were larger than several thousand, only weak and/or unstable signals of REE ions were obtained even if the samples were heated up to very high temperature. It is considered that the presence of an overwhelming number of major element ions (particularly Ca^+) competes with and suppresses the ionization of more refractory and less electropositive elements like the REE (the "matrix problem"). Hence, it is necessary to burn off (at least to some degree) the major elements from loaded samples before heating them up for REE measurements.

After many trials, we concluded that the prolonged heating (preheating) of samples at low temperatures below the REE run temperatures for 5–8 h (depending on the heating temperatures) can eliminate partially but not sufficiently the matrix interferences in question. Preheating too long, however, causes the filament to become brittle and lose sample. We then found that a timely flash heating (raising the evaporation filament current by 0.5 A for a short time) after the preheating can exhaust the major interfering species efficiently without significant loss of REE and then make REE signals sufficiently intensive. However, it must be cautioned that, because of too high temperature, once a specific REE signal (normally the most volatile REE Yb^+ in a double-filament and LaO^+ in single-filament ion source) starts growing, many other REE ions increase almost simultaneously and then decay in a short period if the filament current is left high. Therefore, the filament current must be lowered with the increase of Yb^+ or LaO^+ signals until the signals are gradually stabilized and the filament current approaches the normal condition. In order to process the flash-heating safely, the Ca^+ ion as well as Yb^+ or LaO^+ must be also monitored carefully during flash heating.

Applying the flash heating for 3–10 min, we have finally overcome the major difficulties of the matrix problem. As noted in Table II, the flash heating is most effective for analyses of the most volatile REE (Yb for double filament and La for single filament) but also useful for other elements.

(2) Suppression of Isobaric Interferences in DL-IDMS. The second major problem in DL-IDMS of REE is, similarly to conventional IDMS, the monoxide interference among REE. As discussed previously (*18*, *19*), interferences of GdO^+ to Yb^+, and vice versa, BaO^+ to Eu^+ and LaO^+ and SmO^+ to Er^+ are the long-recognized problems. Beside these problems we often encountered interferences of $BaCl^+$ to Yb^+ and CsO^+ to Sm^+. Among these interferences, the Ba problem is most serious, particularly for high Ba samples like BCR-1. However, they are thought to be variations of common problems in conventional REE mass spectrometry with which we have much experience in this laboratory.

For a double-filament the pressure of the mass spectrometer source is normally maintained to $<10^{-7}$ Torr without any adjustment. The most thermal REE ions in question are observed mainly in metallic form, excepting that Ce exists mainly in monoxide form. Thus, many REE such as Nd, Sm, Eu, Er, Yb, and Lu are measured in metallic form by the double-filament run. Only Ce is measured mostly in monoxide form by a double filament. In this case, the pressure of the ion-source chamber is adjusted to 5×10^{-7} torr by using the oxygen (or air) regulator to obtain a better intensity of CeO^+. This procedure may potentially reduce Gd^+ ion, although we have obtained no sign of Gd^+ ion during the Ce runs. However, if the ion source pressure is not sufficiently good, GdO^+ interference to Yb^+ can occur during Yb run. Occasionally, we recognized signs of $BaCl^+$ and CsO^+ interferences to Yb^+ and Sm^+, respectively, but they could be reduced to undetectable levels by controlling filament current and the ion source pressure. Also the use of HNO_3 instead of $HClO_4$ and HCl throughout all processes helped in partially solving the BaCl problem. All other metals beside REE are measured in metallic form by a double filament (see Table II).

For a single-filament run, the pressure of the ion-source chamber is raised to $(0.5–5) \times 10^{-6}$ Torr. Many REE are now observed mainly in monoxide form. But the CeO^+ signal is rarely identified when a Re single filament is used. Only europium and Yb are observed mainly in metallic form at low temperatures. The Yb^+ ion is normally not stable enough to obtain the best analyses but persistently interfered with GdO^+ at higher temperatures to a minor but significant degree. The BaO^+ and Sm^+ sometimes appear at the early stage of a LaO^+ run but normally can be suppressed by controlling the preheating temperature and the ion source pressure. The best pressure for LaO^+ and NdO^+ is $(0.5–1) \times 10^{-6}$ Torr. On the other hand, the higher pressure ($(1–5) \times 10^{-6}$ Torr) is favored for GdO^+, DyO^+, and ErO^+ intensities. Gadorinium is quite sensitive to oxygen partial pressure and thus several orders of magnitude stronger intensity of GdO^+ is achieved by an increase of the pressure from $<10^{-7}$ to 5×10^{-6} Torr.

In Table II, interfering and monitored isotopes are shown. In order to detect these interferences and to reach the best run condition for the elements, we have monitored two to three elements including interfering elements before and during the data acquisition. The corrections of GdO^+ interference to Yb^+, and vice versa, are normally limited to 1% or less. The other

Table II. Summary of Direct-Loading Mass Spectrometry for (50 μg size) Chondritic Materials

	chemical species measd	spike isotopes	preheating currents, A: center	preheating currents, A: side	time, h	data acquisition currents, A: center	data acquisition currents, A: side	multiplier intensity,[d] A	ratios measured	interfering isotopes	isotopes monitored
					Double-Filament Mode (Pressure ≤1 × 10^{-7} Torr)						
1[a]	K	^{41}K	2.0	0	0.5–1	2.2	0.1–0.2	1 × 10^{-8}	41/39		
2	Rb	^{87}Rb				2.2	0.2–0.3	1 × 10^{-9}	87/85	^{87}Sr	^{86}Sr
3	Ba	^{136}Ba	(3.0	0.3	1)	3.5	0.3–0.4	1 × 10^{-9}	136/138	^{138}La	^{139}La
4	Mg	^{25}Mg	3.5	0.3	1.5	4.0	0.4–0.5	1 × 10^{-9}	25/24		
5	Sr	^{84}Sr				4.0	0.4–0.6	1 × 10^{-9}	84/86		
6	Ca	^{44}Ca				4.0	0.6–0.8	4 × 10^{-8}	44/40	^{40}K	^{41}K
7	Fe	^{54}Fe	3.5	1.2	2–3	4.0[b]	1.3–1.5[b]	(10^{-8})	54/56, 54/52	^{56}Cr, ^{56}(CaO)	^{54}Cr
9	Yb	^{171}Yb	3.5	1.8	5–8	4.0[b]	1.9–2.1[b]	1 × 10^{-11}	171/172, 171/173	^{171}(BaCl + GdO), ^{172}(BaCl + GdO)	^{175}(BaCl)
									171/174	^{173}(BaCl + GdO), ^{174}(BaCl + GdO)	
8	CeO	^{142}Ce				4.0	1.5–1.8	4 × 10^{-10}	158/156, 158/159	^{158}(NdO)	^{159}(NdO), ^{160}(NdO)
10	Eu	^{151}Eu				4.0	2.0–2.1	1 × 10^{-10}	151/153	^{151}(BaO), ^{153}(BaO)	^{152}(Sm + BaO) ^{149}Sm
11	Sm	^{149}Sm				4.0[b]	2.1–2.2[b]	4 × 10^{-11}	149/147	^{149}(CsO)	
12	Nd	^{145}Nd				4.0	2.2–2.3	4 × 10^{-10}	145/146		
13	Er	^{167}Er				4.0[b]	2.3–2.5[b]	4 × 10^{-11}	167/168, 167/170	^{168}(SmO)	^{170}(Er + SmO)
14	Lu	^{176}Lu				4.0	2.3–2.5	1 × 10^{-11}	176/175, 176/174	^{176}(Yb + GdO)	^{173}(Yb + GdO)
									176/173		^{174}(Yb + GdO)
					Single-Filament Mode (Pressure Adjusted to (1–5) × 10^{-6} Torr)						
1	LaO	^{138}La	1.8		6–8		2.1–2.2[c]	1 × 10^{-9}	154/155, 154/152	^{154}(BaO + CeO + Sm)	^{149}Sm, ^{162}(CeO)
											^{152}(Sm + Ba)
2	NdO	^{145}Nd					2.1–2.2	1 × 10^{-9}	161/162		
3	GdO	^{157}Gd					2.2–2.3[c]	1 × 10^{-10}	173/171, 173/172	^{171}(Yb + BaCl), ^{172}(Yb + BaCl)	^{170}Yb
									173/174	^{173}(Yb + BaCl), ^{174}(Yb + BaCl)	^{175}(BaCl)
4	DyO	^{163}Dy					2.2–2.3	4 × 10^{-11}	179/180, 179/182	^{180}(Er*o*)	^{182}(ErO)

[a] Data collection sequence. [b] Flashed at 2.5 A (side) and 4 A (center). [c] Flashed at 2.5 A. [d] Gain = 1 × 10^4 at 2 kV.

corrections are less than 2% in most cases but reach 5–10% for correction of $^{154}Sm^+$ to $^{154}(LaO + Sm)^+$ in some cases.

(3) Heating Schedule and Data Collection. The best run condition of DL-IDMS depends mainly on sizes of samples loaded on filaments, chemical compositions (particularly Na, Ca, Al contents), and REE concentration levels. A typical example of data collection sequence and heating condition (preheating, flash heating, and incremental heating currents) for a 50 μg size chondritic material was shown in Table II.

For a double-filament run, after analyses of alkali metals, alkaline-earth metals, and iron, the sample is preheated at 1.5 A (side) and 3.5 A (center) for 5–8 h and flashed at 2.5 A (side) and 4.0 A (center) until the Yb^+ signal increases sufficiently (normally grow to 10^{-12} A at the detector current within 10 min). Then the side-filament current is dropped to 1.9–2.1 A gradually, keeping the Yb^+ signal stable, and data acquisition is started. With the incremental increase of the side filament current the Yb^+ intensity grows to 10^{-11} A and then decays to the lower intensity, normally in 30 min. Therefore, the Yb mass spectrometry must be completed in this period. Following the heating schedule shown in Table II after Yb analyses, the other REEs are successively analyzed by raising the side-filament current gradually (incremental heating) in the range of 2.0–2.5 A. Since other REE ions are much more stable compared with the Yb^+ ion, we normally spend one hour collecting data for every REE.

For a single filament run, the sample is preheated at 1.8 A for 5–8 h (or overnight) and flashed at 2.5 A. The Eu^+ and LaO^+ signals appear almost at the same time and are most stabilized at 2.0–2.1 A. Once LaO^+ ion is stabilized, data collection can then be continued for 1–2 h. After LaO^+ measurement, stable signals (for 1–2 h) of NdO^+, GdO^+, and DyO^+ (also ErO^+ and LuO^+ sometimes) are also successively measured by incremental raising of filament current to 2.1–2.5 A.

Normally, for analyses of 17 elements of one sample, it takes 2 full days (48 h) for mass spectrometry including preheating time. The preheating and flash heating, however, can be processed complementarily and the total run time is substantially shortened from 48 to 30 h. For example, in a single-filament run, REE analyses can be carried out after "flash heating" (or "preheating") of sample at 2.3–2.5 A for 1–3 h. At the early stage of this work, we failed to determine some REE such as La, Yb, Lu, or Sm occasionally. Since then we improved DL-IDMS in many details, and more recently unsuccessful determination of these elements are limited to less than 10% for analyses of >50 μg size samples. We are now able, on a routine basis, to obtain sufficiently precise REE isotopic ratios with no or correctably small isobaric interferences, even for a few tens of microgram sizes of chondritic materials, which is not too much different from the conventional IDMS.

(4) Analytical Precision and Accuracy. Table III shows results of IDMS analyses with and without chemical separation for the same spiked solutions of the Allende meteorite and U.S. Geological Survey standard rock BCR-1. The conventional IDMS data obtained in this work for BCR-1 are in good agreement with our previous analyses (*15*) and also, in general, with the 1982 consensus values presented by Gladney et al. (*20*). As shown in Figure 2, our REE data for BCR-1

Table III. Comparison of Results by Direct-Loading and Conventional IDMS Analyses for the Same Aliquot Solutions of the Allende Meteorite and BCR-1 Standard (Concentrations Are Given in ppm)[a]

	BCR-1 standard					Allende meteorite			
	DL-IDMS (5-μg samples)			conventional IDMS		DL-IDMS[d]		conventional IDMS	
	1	2	3	30000–250000[b]	1982 consensus values[c]	(1) (50 μg	(2) 80 μg	(1) 16500 μg	(2) 7700 μg
La	24.5	25.2	25.1	25.07 ± 0.16	25.0 ± 0.8	0.444	0.457	0.445	0.445
Ce	54.7	53.8	53.3	54.3 ± 0.3	53.7 ± 0.8	1.208	1.192	1.209	1.201
Nd	28.83	28.79	28.93	29.17 ± 0.10	28.7 ± 0.6	0.911	0.905	0.911	0.904
Sm	6.72	6.87	6.86	6.63 ± 0.03	6.58 ± 0.17	0.300	0.297	0.300	0.299
Eu	1.99	1.95	2.00	1.981 ± 0.011	1.96 ± 0.05	0.1049	0.106	0.1050	0.1050
Gd	6.62	6.71	6.78	6.796 ± 0.015	6.68 ± 0.13	0.365	0.359	0.361	0.359
Dy	–	6.70	6.54	6.52 ± 0.05	6.35 ± 0.12	0.430	0.439	0.433	0.433
Er	3.80	3.84	3.84	3.73 ± 0.03	3.61 ± 0.09	0.294	0.286	0.292	0.291
Yb	0.38	–	3.33	3.383 ± 0.009	3.39 ± 0.08	0.295	0.297	0.298	0.295
Lu	–	0.519	0.501	0.501 ± 0.003	0.512 ± 0.025	–	–	0.0469	0.0463

[a] Sample weight was calculated from the weight of split of aliquot taken. [b] Means of three separate analyses through chemical separation of REE with cation-exchange resin columns. Error limits are twise the standard deviation of the mean. [c] 1982 consensus values presented by Gladney et al. (*20*). [d] Results for other elements (concentrations in ppm): (1) Ba, 4.511; Sr, 14.39; Rb, 1.032; K, 359.1. (2) Ba, 4.537; Sr, 14.79; Rb, 1.035; K, 358.6.

Table IV. Results for DL-IDMS Analyses of the Constituents of Chondrites (Concentrations Are Given in ppm)

	Bjurböle (L4)	Khohar (L3)					
		chondrule				matrix	bulk[d]
	chondrule[c] no. 8 BO[a] 19 μg[b]	no. 1 POP 98 μg	no. 2 RP 66 μg	no. 4 RP 54μg	no. 5 RP 332 μg	6 μg	74500 μg
La	0.235	0.845	0.411	0.456	0.172	1.0	0.422
Ce	0.518	2.24	–	1.08	0.510	20.5	2.72
Nd	0.270	1.52	0.766	0.770	0.322	1.3	0.673
Sm	–	0.494	0.243	0.235	0.108	0.33	0.216
Eu	0.153	0.176	0.091	0.110	0.063	0.10	0.0924
Gd	0.148	0.638	0.359	0.332	0.158	0.53	0.366
Dy	0.252	0.738	0.398	0.385	0.199	0.50	0.356
Er	0.189	0.495	–	0.251	0.125	0.38	0.288
Yb	0.216	0.479	0.260	–	0.131	0.36	0.241
Lu	0.0413	0.075	0.040	–	0.0210	0.058	0.0340

[a] Petrographic types of chondrules: BO, barred olivine; POP, porphyritic olivine and pyroxene; RP, radial pyroxene. [b] Sample size used for analysis. [c] Results for other elements: Ca, 2.00%; Mg, 19.1%; Sr, 28.7 ppm; Rb, 2.94 ppm; K, 600 ppm. [d] Analyzed by conventional IDMS through chemical separation.

show deviations of mostly less than ±2% from the consensus values with mean deviation of +1 ± 1% but with deviations of Dy and Er outside the cited errors. From an inspection of many IDMS REE data for BCR-1 from other institutions, data obtained by Beer et al. (*21*) and Thirlwall (*19*) are considered to be most consistent with ours. Again our values show systematic differences of +1.1 ± 0.5% from data by Beer et al. and +0.7 ± 0.5% from data by Thirlwall. These systematic deviations could be understood as due to variations in the amount of absorptive water in BCR-1 at the different institutions.

In parts b and c of Figure 2, the data obtained by DL-IDMS analysis are compared with those by conventional IDMS for splits taken from the same spiked solutions of BCR-1 and Allende. The REE data by DL-IDMS on the 5 μg size BCR-1 standard are in agreement within mostly ±2–3% with those obtained by conventional IDMS of much larger samples. The REE concentrations in Allende obtained on 50–80 μg samples by DL-IDMS are in agreement within ±1–2% with those obtained by conventional IDMS. Hence, no specific errors due to DL-IDMS are recognized here.

From the above consideration, it is suggested that accuracies of REE determinations by conventional IDMS in this work are comparable to those by Beer et al. and Thirlwall. For DL-IDMS analyses of small meteorite components (in Tables IV and V), the precisions may be 1–3% for most REE (up to 5%) except for some cases mentioned later. It is pointed out that the precision of isotopic analyses on more than 50 μg does not necessarily depend on sample size but mainly on whether the heating schedule was appropriate or not and thus data for smaller sample sizes do not necessarily have poorer precisions.

Table V. Results for Mineral Fragments of Achondrites (Concentrations Are Given in ppm)

	Nakhla	ALH-765			
		plagioclase	pyroxene		
	mesostasis[b] 57 μg[a]	white[c] 1200 μg	dark brown[c] 2520 μg	yellow 93 μg	normalization factor[d]
La	19.78	1.15	3.45	–	0.253
Ce	49.05	2.83	6.04	1.25	0.645
Nd	24.9	1.21	8.17	0.269	0.476
Sm	4.42	–	2.56	0.117	0.154
Eu	1.46	1.45	0.445	0.0406	0.0587
Gd	3.89	0.288	3.35	0.23	0.204
Dy	3.02	0.289	3.73	0.363	0.252
Er	1.66	0.200	2.28	0.339	0.166
Yb	–	0.203	2.12	0.50	0.168
Lu	0.164	0.0164	0.318	0.100	0.0253

[a] Sample weight used for analysis. [b] Results for other elements: Ca, 5.67%; Mg, 2.29%; Ba, 611 ppm; Sr, 550 ppm; Rb, 31.4 ppm; K, 11320 ppm. [c] Analyzed by conventional IDMS through chemical separation. [d] Data from the Orgueil (CI) chondrite (*15*).

For analyses of chondritic samples smaller than 10 μg, the blank contribution during the acid decomposition procedure and the cross-contamination from the Ca–Mg–Fe spike solution were larger than 50% for La and Ce. This causes large uncertainties in the concentrations of light REE. In addition,

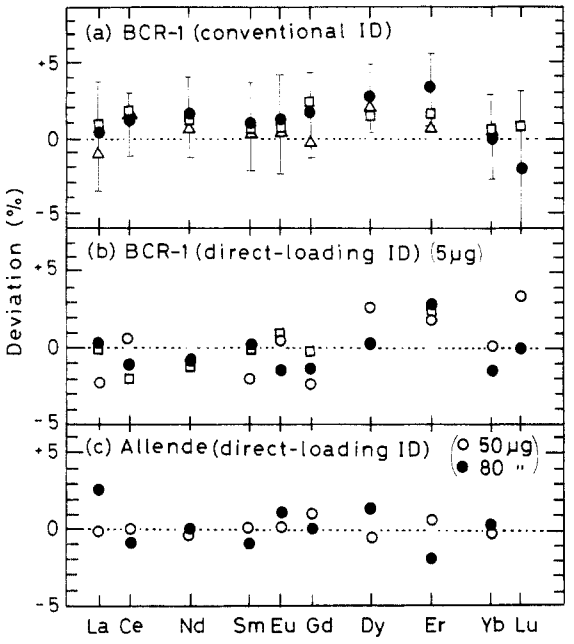

Figure 2. (a) Comparison of conventional IDMS data for BCR-1 obtained in this work with those by Glandney et al. (*20*) (full circles with error bars) (1982 consensus values), Beer et al. (*21*) (open squares) and Thirlwall (*19*) (open triangles). (b) Comparison of DL-IDMS data on 5 μg size BCR-1 with conventional IDMS data obtained for BCR-1 with much larger size (different symbols represent separate analyses). (c) Comparison of DL-IDMS data obtained on aliquot solution (equivalent to 50 μg [open circles] and 80 μg [full circles]) with conventional IDMS analyses for an aliquot (equivalent to 16.5 mg) taken from the same spiked solution of the Allende meteorite.

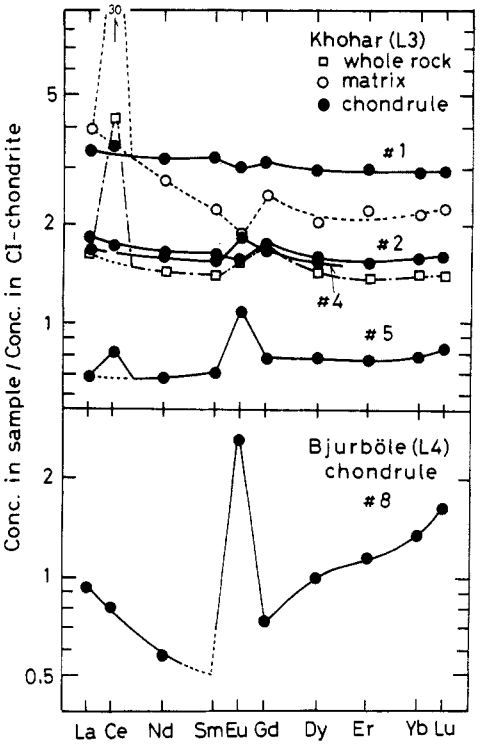

Figure 3. (a) REE abundance patterns for the bulk and constituent materials of the unmetamorphosed ordinary chondrite Khohar (L3). REE abundances are normalized to those in the Orgueil (CI) chondrite (Table V) element by element and plotted against atomic number. Chondrules show flat REE patterns with almost no Ce anomaly but matrix shows large positive Ce anomaly. (b) The REE pattern of the condrule from the metamorphosed ordinary chondrite, Bjurbole (L4), indicating a large Eu anomaly produced by metamorphic activities on plagioclase.

weighing errors (±1 μg) are also significant for these samples, although we are mostly concerned with relative REE abundances and thus weighing errors are not too important. Hence, the lower limit on the precise REE analysis by the direct-loading technique is 10–20 μg on silicate samples with chondritic REE concentration levels but may be less than 5 μg on samples with higher REE contents like BCR-1. The smallest sample of Khohar matrix (6 μg) was at the limit of our analytical capability (see Table IV).

(5) DL-IDMS Analyses for Chondrule and Matrix Materials. Earlier, we have reported significantly large REE fractionations among chondrules from the Allende and Felix carbonaceous chondrites (*13*, *14*). For the purpose of further investigations into the REE characteristics of components of ordinary chondrites, DL-IDMS analyses of chondrule and/or matrix materials from the unmetamorphosed Khohar (L3) and metamorphosed Bjurböle (L4) chondrites were carried out together with conventional IDMS of the bulk Khohar. Results are given in Table IV and Figure 3.

As mentioned earlier, we first tested DL-IDMS by using some chips of a Khohar chondrule (no. 1). The DL-IDMS REE data shown here have been obtained after several unsuccessful trials. As previously reported (*22*) and confirmed by the present work, the bulk Khohar meteorite has a large Ce anomaly (Figure 3a). We first attempted to find any specific component in the meteorite that might bear the large Ce enrichment. The Kohar chondrules show almost flat REE patterns and indicate clearly more or less minor irregularities of Eu and Ce, which cannot, however, substantiate the large Ce anomaly in the bulk sample. On the other hand, the matrix sample shows a large positive Ce anomaly, even larger than that of the bulk sample. Because of a too small sample size, the REE (except for Ce) data of the matrix material are, in general of rather poor quality. The large positive Ce anomaly (Figure 2a), however, may be real. Thus, it is possible that the large Ce anomaly observed for the bulk meteorite was due to the matrix material with Ce enrichment.

The DL-IDMS analyses for a barred olivine type chondrule (no. 8) from Bjurböle (L4) were carried out rather successfully. Since the sample size used for analysis was only 19 μg, contributions of procedural blanks were relatively large: 20% for La, 5% for Ce, and <4% for Nd and other REE. Sm was lost because the content was too low (the estimated content = 2.5×10^{-13} g). Even if some variations of blank contributions are allowed, the REE data obtained here are considered to be precise enough to evaluate the general REE pattern. The highly fractionated REE pattern with a V shape and a large positive Eu anomaly is quite in contrast with the flat REE patterns for chondrules of Khohar. The large positive Eu anomaly and gradual enrichment of heavy REE are explainable as mineral effects of plagioclase and olivine, respectively. In view of the petrologic type 4 of the meteorite, REE abundances in this chondrule are interpreted to have been established during metamorphic activity in a planetary body rather than in the nebula.

(6) DL-IDMS Analyses for Mineral Fragments. Nakhla is one of the basaltic meteorites, the possible Martian origin of which is currently debated. One of the important arguments is focused on the distinctively fractionated REE patterns for the bulk Nakhla. The meteorite consists of cumulus mineral phases (olivine and pyroxene) and minor intercumulus magmas which might carry high REE contents controlling the bulk REE pattern. We collected interstitial (fine-grained) mesostasis thought to represent the intercumulus magma and analyzed them by DL-IDMS. As shown in Table V and Figure 4a, the material shows marked REE fractionations in relative and absolute abundances reported for meteoritic materials (*23*) (even more fractionations compared with BCR-1). Because the sample is rich in alkali

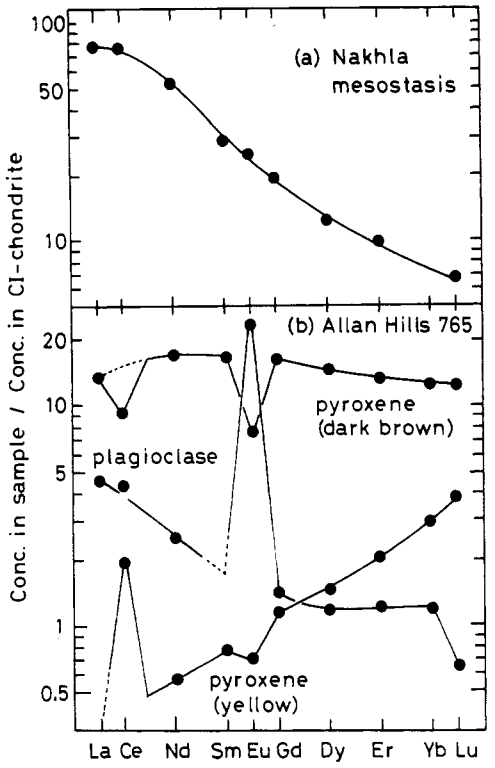

Figure 4. (a) The REE pattern for Nakhla mesostasis representing the late stage magma. (b) REE patterns of mineral grains from the Antarctic meteorite Allen Hills 765.

metals, Ca, and possibly Al (see a footnote of Table V) compared with chondritic materials, application of DL-IDMS to the sample requires more cautions. The analysis was, in general, relatively successful but Yb was lost. In addition, minor deviations of some data points from the smooth curve may cause error. The extreme enrichment and fractionation of incompatible elements observed here suggest that a highly fractionated REE pattern for the bulk meteorite is virtually a reflection of minor interstitial liquid and that the interstitial mesostasis represents a final stage magma after crystallization of the major minerals.

Allan Hills 765 is a basaltic meteorite collected from a bare-ice sheet in Antarctica. In order to examine detailed REE features, particularly Ce anomaly of the bulk meteorite (*24*), we analyzed individual mineral grains by DL-IDMS and conventional IDMS techniques. The mass spectrometries of these samples were, in general, successful but we lost analyses of Sm in plagioclase and La in pyroxene (yellow) because of unreasonable heating processes of these samples. Pyroxene (pigeonite) shows a light REE depleted pattern (possibly with a large positive Ce anomaly) (Figure 4b). On the other hand, the dark brown material (pyroxene) shows a rather flat and higher REE abundance pattern with significant large negative Ce and Eu anomalies. A plagioclase grain shows normal REE distribution except for somewhat irregular distribution of Lu. In view of our analytical precisions of Lu and other heavy REE, the significantly large Lu irregularity observed here is considered to be real. Although the presence of Lu irregularity in planetary materials has not been well documented, Haskin et al. (*25*) have claimed that some lunar anorthosites showed unexplained Lu anomaly. The heterogeneous distributions of Ce irregularity and anomalous distribution of Lu observed for minerals of the Antarctic meteorite are rather rare findings and may require further investigations to reach sufficient interpretation.

CONCLUSION

The DL-IDMS techniques described in this work permit high precision analyses of REE in tiny terrestrial and meteoritic materials as small as 5 μg, such as the USGS standard rock BCR-1 and individual chondrules, the matrix material, and mineral grains of meteorites. As demonstrated here and previously, the technique has revealed the presence of highly fractionated REE patterns for chondrules which have not been clearly detected by other techniques. Such REE features of chondrules from most primitive meteorites represent a marker signiture of high temperature nebular processes in the early solar system (or in a steller environment) and have significant implications for physicochemical conditions at a certain stage of solar system formation. Furthermore, the direct detection of an extremely fractionated REE component or specific REE anomalies in mineral grains from differentiated meteorites indicate a further applicability of the technique to highly fractionated planetary materials.

This technique requires in general more time and caution in the mass spectrometric processes compared with normal IDMS techniques but saves us from an elaborate chemical separation of REE as well as contamination during chemical processing and thus has advantages specifically for REE analyses on tiny planetary materials (<1 mg) with chondritic or lower REE levels. The technique may be potentially applied to a few micrograms or even to submicrogram size cosmic materials for REE analyses if procedural blanks are more reduced.

ACKNOWLEDGMENT

N.N. is grateful to A. Masuda of the University of Tokyo for support during the early stage of this work. The mass spectrometer devices with which we were able to establish the DL-IDMS technique had been transferred from the Geological Survey of Japan to Kobe University. We thank H. Kurasawa and K. Shibata of the Geological Survey of Japan for the machines. We are indebted to R. Hutchison of the British Museum (National History) for providing us with specimens of the Nakhla meteorite, to C. B. Moore of Arizona State University for Khohar specimens, and to K. Yanai of NIPR (Japan) for the ALH-765 meteorite.

Registry No. La, 7439-91-0; Ce, 7440-45-1; Nd, 7440-00-8; Sm, 7440-19-9; Eu, 7440-53-1; Gd, 7440-54-2; Dy, 7429-91-6; Er, 7440-52-0; Yb, 7440-64-4; Lu, 7439-94-3; K, 7440-09-7; Rb, 7440-17-7; Ba, 7440-39-3; Mg, 7439-95-4; Sr, 7440-24-6; Ca, 7440-70-2; Fe, 7439-89-6; pigeonite, 19496-20-9.

LITERATURE CITED

(1) Masuda, A. *Geochem. J.* **1966**, *1*, 11–26.
(2) Schnetzler, C. C.; Thomas, H. H.; Philpotts, J. A. *Anal. Chem.* **1967**, *39*, 1888–1890.
(3) Gast, P. W.; Hubbard, N. J.; Wiesmann, H. Proceedings of the Lunar Science Conference, 11th. *Geochim. Cosmochim. Acta, Suppl.* **1970**, *2*, 1143–1163.
(4) Masuda, A.; Nakamura, N.; Tanaka, T. *Geochim. Cosmochim. Acta* **1973**, *37*, 239–248.
(5) Conard, R. L.; Schmitt, R. A.; Boynton, W. V. *Meteoritics* **1975**, *10*, 384–387.
(6) Gooding, J. L.; Keil, K.; Fukuoka, T.; Schmitt, R. A. *Earth Planet. Sci. Lett.* **1980**, *50*, 171–180.
(7) Nagasawa, H.; Yamakoshi, K.; Higuchi, H. *Geochem. J.* **1980**, *14*, 1–10.
(8) Zinner, E.; Grozaz, G. In *Secondary Ion Mass Spectrometry (SIMS V)*; Benninghoven, A., Colton, R. J., Simmons, D. S., Werner, H. W., Eds.; Springer-Verlag: Berlin, 1986; pp 444–446.
(9) Shimizu, N.; Richardson, S. H. *Geochim. Cosmochim. Acta* **1987**, *51*, 755–758.
(10) Lee, T.; Papanastassiou, D. A.; Wasserburg, G. J. *Geochim. Cosmochim. Acta* **1977**, *41*, 1473–1485.
(11) Nakamura, N.; Okano, O. *Nature* **1985**, *315*, 563–566.
(12) Nakamura, Y.; Fujimaki, H.; Nakamura, N.; Tatsumoto, M. Proceedings of the Lunar and Planetary Science Conference, 16th. *J. Geophys. Res.* **1986**, *91*, No. B4, D239–D250.
(13) Misawa, K.; Nakamura, N. *Geochim. Cosmochim. Acta* **1988**, *52*, 1699–1710.
(14) Misawa, K.; Nakamura, N. *Nature* **1988**, *334*, 47–50.
(15) Nakamura, N. *Geochim. Cosmochim. Acta* **1974**, *38*, 757–775.
(16) Nakamura, N. Ph.D. Thesis, University of Tokyo, Tokyo, 1975.
(17) Kurasawa, H.; Ando, N.; Shirahase, T.; Naito, M. *Proceedings of the International Conference on Mass Spectroscopy*; Ogata, K., Hayakawa, T., Eds.; University of Tokyo Press: Tokyo, 1970; pp 236–244.

(18) Schumann, S.; Philpotts, J. A.; Fryer, P. *Anal. Chem.* **1979**, *52*, 214-216.
(19) Thirlwall, M. E. *Chem. Geol.* **1982**, *35*, 155-166.
(20) Gladney, E. S.; Burns, C. E.; Roelandts, I. *Geostand. Newsl.* **1982**, *7*, 3-226.
(21) Beer, H.; Walter, G.; Macklin, R. L.; Patchett, P. J. *Phys. Rev. C* **1984**, *30*, 464-478.
(22) Nakamura, N.; Masuda, A. *Earth Planet. Sci. Lett.* **1973**, *19*, 429-437.
(23) Nakamura, N.; Unruh, D. M.; Tatsumoto, M.; Hutchison, R. *Geochim. Cosmochim. Acta* **1982**, *46*, 1555-1573.
(24) Nakamura, N.; Masuda, A. *Mem. Natl. Inst. Polar Res., Spec. Issue (Jpn)* **1980**, *No. 17*, 159-167.
(25) Haskin, L. A.; Lindstrom, M. M.; Salpas, P. A.; Lindstrom, D. J. *Proc. Lunar Planet. Sci.* **1981**, *12B*, 41-46.

RECEIVED for review August 5, 1988. Accepted January 4, 1989.

Ultramicroelectrode Ensembles. Comparison of Experimental and Theoretical Responses and Evaluation of Electroanalytical Detection Limits

I. Francis Cheng, Lisa D. Whiteley, and Charles R. Martin*

Department of Chemistry, Texas A&M University, College Station, Texas 77843-3255

In a recent correspondence, we described a new procedure for preparing ultramicrodisk electrode ensembles; the ultramicrodisks were formed by filling the pores of a microporous host membrane with carbon paste. In this paper we present results of quantitative and semiquantitative analyses of the electrochemical response characteristics of these ultramicroelectrode ensembles; we show that the responses are in agreement with predictions of established electrochemical theory. We also show that one of the ensembles investigated here can yield electroanalytical detection limits that are an order of magnitude lower than detection limits at an equivalent macrosized (0.331 cm^2) electrode.

INTRODUCTION

We have recently described a new method for preparing ensembles of ultramicrodisk electrodes (*1-3*); the ultramicrodisks are prepared by filling the pores of a microporous host membrane with an electronically conductive material. Thus, the pores in the host membrane act as templates for the elements of the ultramicroelectrode ensemble (*1-3*). This procedure has been used by us and others to prepare Pt, Au, and carbon paste based ultramicrodisk ensembles (*1-4*).

We have conducted quantitative and semiquantitative analyses of the electrochemical response characteristics of carbon paste based ensembles prepared by using the microporous membrane method. These analyses have shown that the electrochemical response characteristics of these ensembles are in agreement with the predictions of established electrochemical theory. Furthermore, we have shown that these ensembles yield electroanalytical detection limits that are lower than detection limits obtained at analogous macrosized carbon paste electrodes. We report the results of these and related investigations here.

EXPERIMENTAL SECTION

Reagents. $Fe(bpy)_3(ClO_4)_2$ (G. F. Smith), $K_4Fe(CN)_6$ (Aldrich), H_2SO_4 (Fisher), and K_2SO_4 (Fisher) were used as received. Purified water was obtained by passing house-distilled water through a Millipore Milli-Q water purification system. Carbopack C carbon particles (Supelco, 80/100 mesh) and high vacuum grease (Dow Corning) were used to prepare the carbon paste.

Membranes. Microporous membranes were obtained from the Nuclepore Corp. Table I lists nominal and experimentally determined parameters for these membranes. Nominal values were provided by Nuclepore. Experimental pore diameters were obtained by manually measuring pores in high-resolution electron micrographs of the membranes. Electron microscopic and electrochemical methods were used to obtain experimental pore densities. The electron microscopic method involved counting the pores in low-resolution electron micrographs of the membranes. The electrochemical method will be discussed below. The average (center-to-center) distance between pores (d) was calculated via (*5*)

$$d = 0.5q^{-1/2} \quad (1)$$

where q is the pore density (pores cm^{-2}).

Electrodes and Instrumentation. Carbon paste was prepared by mixing equal weights of carbon powder and high-vacuum grease (*3*). Macrosized carbon paste electrodes (area = 0.331 cm^2) were prepared by using the conventional procedure (*6*). Ensembles were prepared by rubbing carbon paste into and through the Nuclepore membranes (*3*). The carbon paste impregnated membrane was then applied to the fact of a macrosized carbon paste electrode (*3, 6*). Ensembles were prepared from membranes with measured pore diameters of 13, 8, and 3 μm (Table I); these ensembles are designated 13UME, 8UME, and 3UME.

Nuclepore membrane has a dull and a shiny face; the dull face was applied to the substrate electrode (*3*). We reported previously that the shiny face results from polishing (*3*); we have since learned that this is incorrect (*7*). Nuclepore membranes are prepared from solution-cast polycarbonate film (*7*). The dull face is the side that had been exposed to the casting surface; the shiny face is the side that had been exposed to air during solvent evaporation (*7*).

A one-compartment electrochemical cell, a Ag/AgCl reference electrode, and a carbon rod counter electrode were employed. Either 0.70 M K_2SO_4 or 0.5 M H_2SO_4 served as the supporting electrolyte. The electrochemical instrumentation has been described previously (*2, 3*). Photomicrographs were obtained by using a Bausch and Lomb StereoZoom microscope.

Electrochemical Experiments. Cyclic voltammetry was used to evaluate the response characteristics of the ensembles. Peak currents from high scan rate voltammograms were quantitatively analyzed by using theory developed by Osteryoung et al. (*8*). Details will be presented in Results and Discussion. These quantitative analyses provided the electrochemical pore densities shown in Table I.

RESULTS AND DISCUSSION

Membrane Characterizations. Table I compares nominal and experimentally determined pore diameters and densities. Two independent methods were used to determine the experimental densities, and the agreement between these methods is quite good (Table I). Table I shows that the experimental densities are significantly less than the nominal

0003-2700/89/0361-0762$01.50/0